

# MULTIGRID RECONSTRUCTION OF SOUND FIELDS USING MOVING MICROPHONES

*Fabrice Katzberg, Radoslaw Mazur, Marco Maass, Philipp Koch, and Alfred Mertins*

Institute for Signal Processing  
University of Lübeck  
Ratzeburger Allee 160, 23562 Lübeck, Germany

## ABSTRACT

A multiresolution technique is presented for sound field recovery based on measurements of one or multiple moving microphones. The interpolation of the spatial samples enables us to set up a system of linear equations that recovers room impulse responses on a virtual uniform grid in space. The spacing of the virtual grid must be very small when directly recovering for the entire bandwidth, thus, the system to be solved requires a large number of measurement positions. In this work, we propose two recovery schemes based on multiple virtual grids that represent distinct subbands of the spatio-temporal sound field. This allows for faster reconstruction of low frequencies at minor computational cost and improves the recovery quality when measurement noise is present.

**Index Terms**— Plenacoustic function, room impulse responses, moving microphones, spatial multigrid, multiresolution scheme

## 1. INTRODUCTION

Acoustic applications that assume free-field environments typically decrease their performance in the presence of reverberation. However, if the information on room impulse responses (RIRs) that describe the sound transfer from the sources to the receivers is given, techniques for listening room compensation can be applied [1, 2, 3].

In order to describe the spatio-temporal sound field, the concept of the plenacoustic function (PAF) [4, 5] has been introduced. This function encapsulates the information on the entire set of spatio-temporal RIRs for any receiver position in space, depending on the constellation of sound sources and the room attributes.

Common approaches for the stationary measurement of RIRs use perfect sequences [6, 7], maximum-length sequences (MLS) [8, 9], and exponential sine sweeps [10]. Applying these signals for excitation enables one to obtain the RIRs by use of simple correlation techniques with low computational demand.

A method for the dynamic measurement of a set of RIRs has been proposed in [11]. Here, the use of one moving microphone allows for the reconstruction of all RIRs along the given trajectory. However, an input signal that is specially designed for the given trajectory is needed, and the speed of the microphone must be constant. In this case, quite different from RIR measurements with a fixed microphone, the excitation signal must not contain all frequencies, but only a certain subset. The omitted frequencies are essentially generated through the Doppler effect. In [12], direction dependent head-related RIRs (HRIRs) are estimated. With a rotating setup, the dynamic procedure is able to reconstruct HRIRs on single circles.

In this work, we propose a multigrid technique that allows for the recovery of the spatio-temporal sound field within a given region of interest. For the subband decomposition of the sound field, successive filtering is applied on the measurement signals given by microphones on a moving array. According to the dispersion relation of propagative sound waves, this filtering in time domain directly affects the frequencies of the spatial domains since the four-dimensional spectrum of sound fields forms a hypercone along the temporal frequency axis [5]. This inherent relationship between time and space domains was also used in [13] for low frequency interpolation of RIRs based on compressed sensing (CS) [14, 15].

Exploiting the structured sparsity of the spectral cone, we model multiple virtual grids with different resolutions in space on which subband room impulse responses are stage-wisely recovered by solving systems of linear equations. These are built up by interrelating the dynamic measurements with the grid RIRs through spatial interpolation as proposed in [16]. For the subsequent subband synthesis, filtering is applied in the spatial domains, in order to obtain the spatio-temporal sound field at full bandwidth.

In total, we present two general schemes for multiresolution recovery. One method successively performs two-band frequency splits in the decomposition step. Consequently, the virtual grid points of any coarser grid with lower resolution in space fit into the sample points of any finer spatial grid by some integer delay. In contrast, the other proposed scheme considers the decomposition into subbands of constant bandwidth, and, thus, considers fractional delays between the uniform grid points of each resolution level. This requires fractional delay interpolation techniques [17] for the subband synthesis step.

## 2. SAMPLING OF SOUND FIELDS

In the following, the concept of the plenacoustic function giving a description of sound fields is outlined, and its sampling and reconstruction are formalized. Further, the inherent relationship between the temporal and spatial dimensions is pointed out, which is the basis for the design of the proposed multiresolution recovery schemes.

### 2.1. The Plenacoustic Function

For a given pair of sound source and listener at fixed positions in space, the time  $t$  dependent room impulse response (RIR)  $h(t)$  describes the received sound resulting from a Dirac pulse emitted at time  $t = 0$ . Assuming the acoustic environment to be linear time-invariant (LTI), for the source signal  $s(t)$ , the observed signal is given by  $x(t) = h(t) * s(t)$ , where the asterisk  $*$  denotes convolution. In order to include spatial dependencies, the plenacoustic function (PAF) has been introduced in [4, 5]. It gathers all RIRs of a room for a given source configuration. The PAF, denoted as  $p(\mathbf{r}, t)$ ,

---

This work has been supported by the German Research Foundation under Grants No. ME 1170/8-1 and ME 1170/10-1.

describes the sound field in space as a function of both time  $t$  and listener position  $\mathbf{r} = [r_x, r_y, r_z]^T$ . For the simplest setup with one single sound source emitting  $s(t)$  at fixed position, the PAF is

$$p(\mathbf{r}, t) = \int_{-\infty}^{\infty} h(\mathbf{r}, \tau) s(t - \tau) d\tau, \quad (1)$$

where  $h(\mathbf{r}, t)$  is the spatio-temporal RIR from the source position to the point  $\mathbf{r}$ . Due to the LTI system model, the PAF for multiple fixed sound sources consists of a sum of integrals as given in (1). Referring to [4, 5], we consider the PAF, without loss of generality, only for the case where a single source at fixed position emits a Dirac pulse at  $t = 0$ . With this,  $p(\mathbf{r}, t) = h(\mathbf{r}, t)$ .

## 2.2. Inherent Connection of the Dimensions

For positions sufficiently far away from the sound source and room walls, evanescent sound waves can be ignored, thus, the dispersion relation

$$k_x^2 + k_y^2 + k_z^2 = \frac{\omega^2}{c_0^2} \quad (2)$$

gives an explicit relationship between the spatial frequencies  $k_x, k_y, k_z$  in  $\text{rad m}^{-1}$  and the temporal angular frequency  $\omega = 2\pi f$  in  $\text{rad s}^{-1}$  [5, 13]. The velocity of the waves is  $c_0 = \omega/\tilde{k}$ , with the angular wavenumber  $\tilde{k} = |\mathbf{k}|$  and the wave vector  $\mathbf{k} = [k_x, k_y, k_z]^T$ . Since air is a non-dispersive medium for frequencies within the human hearing range,  $c_0$  is independent of  $\omega$ . So, the speed of sound is only a function of atmospheric conditions inside the closed room, e.g. temperature and pressure, which are assumed to be constant according to the LTI model. In consequence, (2) provides a direct connection between the temporal and spatial frequencies: the four-dimensional spectrum of the PAF ideally lives on the three-dimensional surface of a hypercone along the temporal frequency axis  $\omega$ . Moreover, when the PAF is bandlimited in time domain to  $\omega_c$ , then it is also bandlimited in the spatial domain by  $\tilde{k}_c = \omega_c/c_0$ .

## 2.3. Uniform Sampling and Reconstruction

Under the assumption that the PAF is bandlimited, it can be reconstructed through equidistant sampling in time and space dimensions. For the uniform sampling in time, let  $T$  denote the sampling interval leading to measurements at sampling points  $t_n = nT$  with  $n \in \mathbb{Z}$  being the discrete time variable. Considering the cutoff frequency  $f_c = \omega_c/2\pi$ , the sampling frequency  $f_s = 1/T$  has to fulfill  $f_s < 2f_c$  according to the Nyquist-Shannon sampling theorem.

The uniform sampling in space requires a Cartesian grid where the equidistant sampling points  $\mathbf{r}_g \in \mathcal{G}$  are given by the set

$$\mathcal{G} = \left\{ \mathbf{r}_g \mid \mathbf{r}_g = \mathbf{r}_0 + [g_x \Delta, g_y \Delta, g_z \Delta]^T \right\}, \quad (3)$$

with the grid origin  $\mathbf{r}_0$  and the discrete grid variables in  $\mathbf{g} = [g_x, g_y, g_z]^T \in \mathbb{Z}^3$ . Following (2), the sampling interval for each space dimension  $x, y, z$  must be  $\Delta < c_0/(2f_c)$  to avoid aliasing.

The ideal reconstruction of the continuous sound field  $h(\mathbf{r}, t)$  from samples  $h(\mathbf{g}, n)$  is accomplished by a 4D sinc filter with infinite support. Since the amplitudes of RIRs decrease exponentially and are assumed to vanish into the noise level beyond  $t_{L-1}$  for given  $f_s$ , finite length interpolation filters achieve reasonable approximations for the time dimension when limiting the temporal sample points to  $n \in [0, L-1]$ . However, due to limited positions  $\mathbf{g} \in G = \{0, \dots, X-1\} \times \{0, \dots, Y-1\} \times \{0, \dots, Z-1\}$  on a finite sampling grid in space, the PAF is rectangularly windowed along the spatial dimensions. Oversampling in space, i.e. using a much finer

grid than demanded by the Nyquist rate, reduces the effect of spatial windowing.

## 3. THE PROPOSED MULTIGRID RECOVERY

We first outline the underlying dynamic sampling procedure described in [16], where a system of linear equations is built up whose solution estimates RIRs on a modeled virtual grid in space. Then, two new multigrid recovery schemes are deduced by exploiting the dispersion relation of propagative sound waves.

### 3.1. Dynamic Sampling Procedure

For the recovery of RIRs  $h(\mathbf{g}, n)$  on a virtual grid  $G$  in space with  $\Delta$  fulfilling the Nyquist-Shannon sampling theorem, we consider a scenario in which a single source emits a pre-defined signal and one or more microphones are moved through the volume of interest while their signals are simultaneously recorded together with the position information. The following description is given for a single moving microphone. The use of multiple microphones is straightforward and allows for a tradeoff between calibration effort and measuring time.

The RIR at any position inside the volume of interest can be computed via interpolation from  $h(\mathbf{g}, n)$ , including the locations on the microphone trajectory. Assuming perfect interpolation and using (1), each sample  $x(n)$  recorded by the microphone at position  $\mathbf{r}(n) = [r_x(n), r_y(n), r_z(n)]^T$  contributes an equation of the form

$$x(n) = \sum_{k=0}^{L-1} \sum_{\mathbf{g} \in G} \varphi(\mathbf{r}(n), \mathbf{r}_g) h(\mathbf{g}, k) s(n-k) + \eta(n), \quad (4)$$

where  $\eta(n)$  is measurement noise and  $\varphi(\mathbf{r}(n), \mathbf{r}_g)$  is an interpolation function weighting the sought RIRs on the modeled grid subject to the displacements  $\mathbf{r}(n) - \mathbf{r}_g$ . Of course, the interpolation is not ideal due to the finite spatial support. However, a dense virtual grid with a sampling frequency well above the Nyquist rate in combination with an interpolation kernel that is maximally flat in the frequency domain may provide sufficient results. By concatenating the  $N = XYZ$  grid RIRs of length  $L$  in vector  $\mathbf{h} \in \mathbb{R}^{N \times L}$  and defining  $\mathbf{x} = [x(0), \dots, x(M-1)]^T$  and  $\boldsymbol{\eta} = [\eta(0), \dots, \eta(M-1)]^T$ , (4) leads to the system of linear equation

$$\mathbf{x} = \mathbf{A}\mathbf{h} + \boldsymbol{\eta}. \quad (5)$$

The matrix  $\mathbf{A}$  has block structure,  $\mathbf{A} = [\boldsymbol{\Phi}_1 \mathbf{S}, \boldsymbol{\Phi}_2 \mathbf{S}, \dots, \boldsymbol{\Phi}_N \mathbf{S}]$ , where  $\boldsymbol{\Phi}_u \in \mathbb{R}^{M \times M}$  is a diagonal matrix stacking the interpolation coefficients of all  $M$  measurements for the  $u$ -th RIR on the virtual grid and  $\mathbf{S} \in \mathbb{R}^{M \times L}$  is the convolution matrix of the source signal. In case the linear system is not underdetermined, its unique least-squares solution yields the estimate of  $h(\mathbf{g}, n)$ .

### 3.2. Multiresolution Approaches

Instead of solving for the entire bandwidth of the PAF, we propose a model of multiple virtual grids in space with different resolutions, leading to multiple linear systems of different sizes. Based on (4), a separate system of linear equations

$$\mathbf{x}^{(v)} = \mathbf{A}^{(v)} \mathbf{h}^{(v)} + \boldsymbol{\eta}^{(v)} \quad (6)$$

is set up for each resolution level  $v \in \{1, \dots, V\}$ , where  $\mathbf{x}^{(v)}$  is the filtered measurement signal of the moving microphone with frequencies  $\omega$  limited to the subband  $\omega_c^{(v-1)} \leq \omega < \omega_c^{(v)}$ . Due to (2),

for lower temporal subbands,  $\mathbf{h}^{(v)} \in \mathbb{R}^{LN^{(v)}}$  may contain a smaller number  $N^{(v)}$  of RIRs on a coarser virtual grid  $\mathbf{g}^{(v)} \in G^{(v)}$  inside the volume of interest. Let  $\Delta^{(v)}$  denote the spatial sampling interval at resolution level  $v$ . The initial spacing  $\Delta^{(1)}$  of the coarsest grid  $G^{(1)}$ , with  $N^{(1)} = 2^d$  RIRs for the  $d$ -dimensional case, covers the entire volume of interest. The positions of the initial RIRs frame the sampling area and are also present on any finer grid for  $v > 1$ . According to (2), the temporal subband limits must be

$$\omega_c^{(v)} \leq \frac{\pi c_0}{\Delta^{(v)}}, \quad (7)$$

in order to avoid spatial aliasing. The lowest bound is  $\omega^{(0)} = 0$ . At the final resolution level  $V$ ,  $\Delta^{(V)}$  is supposed to fulfill the spatial Nyquist-Shannon condition for the broadband cutoff  $\omega_c$ . Due to the finite grid and the Doppler effect, all cutoff frequencies are chosen sufficiently smaller in practice than required by (2).

By decomposing the original large problem (5) into smaller problems (6), the sound field recovery at low frequencies is already possible using a few measurements acquired after a short sampling time. Vice versa, by fixing the sampling time, a coarser virtual grid allows for more dynamic measurements per grid RIR than a finer one, which makes the recovery of low frequencies more robust against noise. Moreover, for trajectories which lead to ill-conditioned or undetermined systems (5), the proposed method allows for a spatial adaptation of the bandwidth to be recovered. Of course, the formulation (6) is suitable to apply CS based techniques reducing the dimensionality of the wanted signal. For example, a frequency representation of the solution vector allows one to explicitly reconstruct frequency quartets on the spectral cone according to (2) which defines the subspace in which the signal actually lives.

### 3.2.1. Half Bandwidth Multigrid (HBM)

We first present a multigrid recovery scheme, referred to as HBM, which is based on cascaded half-band decompositions of the measured signal  $x(n)$ . This allows us to model the virtual grid for each resolution level  $v > 1$  with halving intervals  $\Delta^{(v)} = \Delta^{(v-1)}/2$ , so  $N^{(v)} = (2^{v-1} + 1)^d$ . Thus, the virtual uniform grid in space is successively upsampled by factor two as outlined in Fig. 1(a). The gradual doubling of the temporal subband width,  $\omega_c^{(v)} = 2\omega_c^{(v-1)}$ , is indicated in Fig. 1(b) by exponentially increasing segments of the spectral cone.

Overall, the solutions  $\mathbf{h}^{(v)}$  of the linear systems (6) yield the parts  $h(\mathbf{g}^{(v)}, n)$  of the broadband PAF, each at distinct temporal subbands on spatial grids  $G^{(v)}$  with different resolutions. For synthesis of the subbands, recursive interpolation in space is applied,

$$h(\mathbf{g}^{(v)}, n) = h(\mathbf{g}^{(v-1)}, n) + h(\mathbf{g}_{\uparrow 2}^{(v-1)}, n) * \varphi_0(\mathbf{g}^{(v)}), \quad (8)$$

where  $\mathbf{g}_{\uparrow 2}^{(v)}$  denotes the upsampled virtual grid of level  $v$  by factor two along each spatial dimension and  $\varphi_0(\mathbf{g}^{(v)})$  is a  $d$ -dimensional low-pass filter for interpolating the intermediate positions on the finer grid.

### 3.2.2. Constant Bandwidth Multigrid (CBM)

Given an initial grid  $G^{(1)}$  for the first resolution level as described above, it might be more appropriate to model the more highly resolved grids according to  $\Delta^{(v)} = \Delta^{(1)}/v$  as shown in Fig. 1(c). For level  $v$ , only one more grid position per room dimension is taken into account compared to level  $v - 1$ , so  $N^{(v)} = (v + 1)^d$ . Consequently, grid points on any coarser grid may possess a fractional

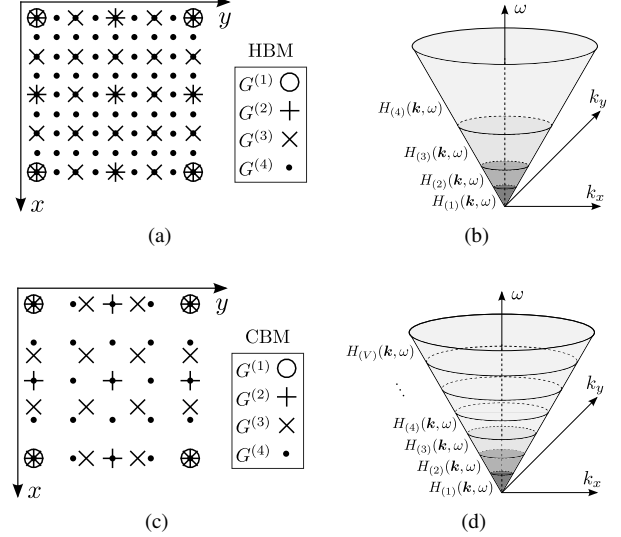


**Fig. 1.** Outline of the virtual grids  $G^{(v)}$  in two-dimensional space and the corresponding PAF subbands  $H^{(v)}(\mathbf{k}, \omega)$  to be recovered for (a)-(b) the HBM method and (c)-(d) the CBM method.

delay referred to the points on any finer grid, i.e. non-uniform interpolation in space is necessary for the subband synthesis step (cf. Figs. 1(a) and 1(c)). This multigrid procedure considers the decomposition of  $x(n)$  into temporal narrow bands with constant bandwidth ( $\omega_c^{(v)} = v\omega_c^{(1)}$ , cf. Fig. 1(d)), and is denoted as CBM.

Defining the interpolated RIR on a finer grid  $G^{(v)}$  by use of samples on a coarser grid  $G^{(l)}$  as

$$\tilde{h}_l(\mathbf{g}^{(v)}, n) = \sum_{\mathbf{g}^{(l)} \in G^{(l)}} h(\mathbf{g}^{(l)}, n) \varphi(\mathbf{r}_{\mathbf{g}^{(v)}}, \mathbf{r}_{\mathbf{g}^{(l)}}), \quad (9)$$

the CBM method with instantaneous subband synthesis by analogy with (8), denoted as CBM1, demands the recursive scheme

$$h(\mathbf{g}^{(v)}, n) = h(\mathbf{g}^{(v-1)}, n) + \tilde{h}_{v-1}(\mathbf{g}^{(v)}, n). \quad (10)$$

Nevertheless, we propose an algorithm with one single synthesis step at the final resolution level  $V$ , in order to avoid that the errors caused by fractional delay interpolation propagate through every subsequent resolution level. This method is named CBM2. It estimates the broadband PAF according to

$$h(\mathbf{g}, n) = h(\mathbf{g}^{(V)}, n) + \sum_{v=1}^{V-1} \tilde{h}_v(\mathbf{g}^{(V)}, n). \quad (11)$$

## 4. EXPERIMENTS AND RESULTS

For the following experiments, we simulated RIRs and microphone measurements by use of the image source method [18], considering a room of size  $5.8 \text{ m} \times 4.15 \text{ m} \times 2.55 \text{ m}$ . The reverberation time  $RT_{60} = 0.3 \text{ s}$  was chosen. The cutoff frequency of the RIRs, limited to length  $L = 1000$ , was  $f_c = 4 \text{ kHz}$ . The position of the sound source was set to  $[1.4, 1.6, 1.0]^T$  in a world coordinate system with unit 1 m. We used 1000 repetitions of an MLS with power  $\sigma_s^2 = 1$  and period length of 1023 as excitation signal. The origin of the virtual grids was set to  $\mathbf{r}_0 = [2.75, 1.4, 0.8]^T$ . The volume of interest

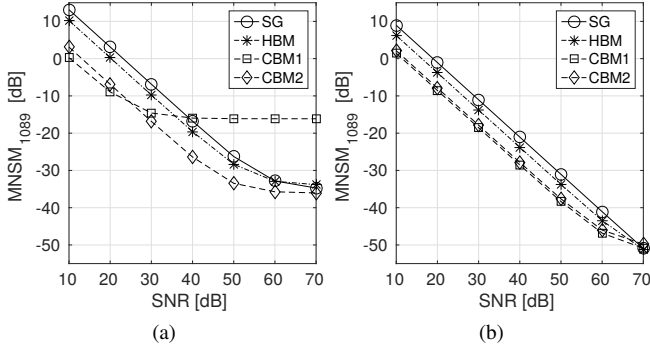


**Fig. 2.** Comparison of PAF quality between the single grid recovery and the proposed multigrid schemes, using (a) the linear interpolator and (b) the Lagrange interpolator for spatial interpolation.

was a plane of size  $0.3 \text{ m} \times 0.3 \text{ m}$ . For the dynamic measurement, a microphone array with four microphones arranged on a quadratic grid with spacing  $0.15 \text{ m}$  was applied. The array performed one period of a Lissajous trajectory [19] covering the plane with frequency ratio  $16/17$ .

We considered the recovery of the PAF on a uniform grid in space with size  $33 \times 33$  and spacing  $\Delta = 0.0094 \text{ m}$  which involves a spatial oversampling by factor  $4.56$ . Accordingly, the HBM scheme performs 6 resolution levels and the CBM method processes 32 subband signals with bandwidth of  $125 \text{ Hz}$ . Hamming windowed band-pass filters of order 1000 were used for the filtering of  $x(n)$ .

As evaluation criterion for the quality of the recovered PAF, we use the mean *normalized system misalignment* [cf. 3, 20]

$$\text{MNSM}_N = \frac{1}{N} \sum_{u=1}^N \frac{\|\mathbf{h}_u - \hat{\mathbf{h}}_u\|_{\ell_2}^2}{\|\mathbf{h}_u\|_{\ell_2}^2}, \quad (12)$$

with  $\mathbf{h}_u \in \mathbb{R}^L$  containing the true RIR and  $\hat{\mathbf{h}}_u \in \mathbb{R}^L$  being the reconstructed RIR at grid index  $u$ . For the frequency analysis, we define the mean energy spectral density of the error, denoted with ME-ESD and calculated as

$$\text{ME-ESD}(f) = \frac{1}{N} \sum_{u=1}^N |H_u(f) - \hat{H}_u(f)|^2, \quad (13)$$

where  $H_u(f)$  and  $\hat{H}_u(f)$  are the Fourier transforms of the true RIR and the corresponding reconstructed RIR, respectively.

The quality of PAF reconstruction compared to the single grid recovery (SG) is presented in Fig. 2 for various signal-to-noise ratios  $\text{SNR} = \sigma_s^2/\sigma_\eta^2$ , where  $\sigma_\eta^2$  is the power of the measurement noise  $\eta(n)$ . For the interpolation of the dynamic measurements and the spatial synthesis of the subbands, we first tested a simple linear interpolator (Fig. 2(a)). Here, the proposed HBM and CBM2 methods achieved an accuracy gain up to 3 dB and 10 dB, respectively, compared to the broadband recovery on one single grid. The CBM1 scheme failed due to poor interpolation quality successively propagating through fractional delayed grids. Further, we tested the Lagrange interpolator which is equivalent to a maximally flat fractional delay filter with finite impulse response [21] and, thus, allows for approximating the ideal interpolation at low frequencies. This led to improvements for all of the proposed multigrid schemes.

There are frequency errors around  $\omega_c^{(v)}$  due to the non-perfect subband decomposition performed by the chosen filters and errors

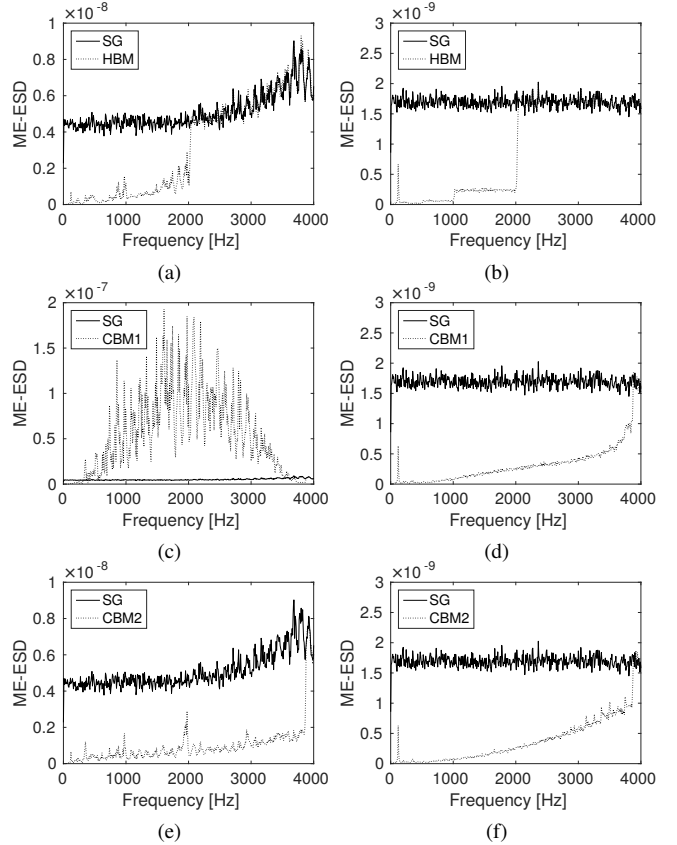


**Fig. 3.** Frequency dependent error for  $\text{SNR} = 50 \text{ dB}$  in comparison between the single grid recovery and the proposed multigrid schemes: On the left-hand side, the linear interpolation was used, the right-hand side shows the results for the Lagrange interpolation. Note in (c) the excessive gap between the error functions for mid frequencies resulting in a very small scaling for the single grid case.

caused by insufficient spatial synthesis (cf. Fig. 3). However, except for the special case CBM1 combined with the linear interpolator (cf. Fig. 3(c)), both error types systematically induced by the multiresolution schemes are clearly below the error level of the SG recovery for  $\text{SNR} < 70 \text{ dB}$  in our setup.

## 5. CONCLUSIONS

In this paper, we presented two general multiresolution strategies for sound field reconstruction. Based on measurements of moving microphones being tracked, stage-wise recovery schemes for a uniform grid in space were proposed. Considering distinct subbands of the spectral cone of sound fields, multiple systems of linear equations were solved for multiple spatial grids with different resolutions. We experimentally showed that the multigrid methods improve the recovery quality under noisy conditions. The methods allow for the spatial adaptation of sound field recovery, i.e. the recovery of locally varying bandwidths depending on the trajectory. This motivates the setup of one hand-held microphone with arbitrary trajectory. CS based methods suited for the proposed multiresolution reconstruction are currently under investigation.

## 6. REFERENCES

- [1] V. N. Mourjopoulos, "Digital equalization of room acoustics," *Journal of the Audio Engineering Society*, vol. 42, no. 11, pp. 884–900, 1994.
- [2] S. Götze, E. Albertin, M. Kallinger, A. Mertins, and K.-D. Kammeyer, "Quality assessment for listening-room compensation algorithms," in *Proc. IEEE International Conference on Acoustics, Speech, and Signal Processing*, 2010, pp. 2450–2453.
- [3] J. O. Jungmann, S. Götze, and A. Mertins, "Room impulse response reshaping by  $p$ -norm optimization based on estimates of room impulse responses," in *Proc. German Annual Conference on Acoustics*, Düsseldorf, Germany, 2011, pp. 611–612.
- [4] T. Ajdler and M. Vetterli, "The plenacoustic function, sampling and reconstruction," in *Proc. IEEE International Conference on Acoustics, Speech, and Signal Processing*, 2003, vol. 5, pp. 616–619.
- [5] T. Ajdler and L. Sbaiz, "The plenacoustic function and its sampling," *IEEE Transactions on Signal Processing*, vol. 54, no. 10, pp. 3790–3804, 2006.
- [6] V. P. Ipatov, "Ternary sequences with ideal periodic autocorrelation properties," *Radio Engineering and Electronic Physics*, vol. 24, pp. 75–99, 1979.
- [7] H.-D. Lüke, "Sequences and arrays with perfect periodic correlation," *IEEE Transactions on Aerospace and Electronic Systems*, vol. 24, no. 3, pp. 287–294, 1988.
- [8] J. Borish and J. B. Angell, "An efficient algorithm for measuring the impulse response using pseudorandom noise," *Journal of the Audio Engineering Society*, vol. 31, no. 7/8, pp. 478–488, 1983.
- [9] D. D. Rife and J. Vanderkooy, "Transfer-function measurement with maximum-length sequences," *Journal of the Audio Engineering Society*, vol. 37, no. 6, pp. 419–444, 1989.
- [10] A. Farina, "Advancements in impulse response measurements by sine sweeps," in *Proc. 122nd Audio Engineering Society Convention*, Vienna, Austria, 2007.
- [11] T. Ajdler, L. Sbaiz, and M. Vetterli, "Dynamic measurement of room impulse responses using a moving microphone," *Journal of the Acoustical Society of America*, vol. 122, no. 3, pp. 1636–1645, 2007.
- [12] Gerald Enzner, "3d-continuous-azimuth acquisition of head-related impulse responses using multi-channel adaptive filtering," *IEEE Workshop on Applications of Signal Processing to Audio and Acoustics*, pp. 325 – 328, 2009.
- [13] R. Mignot, G. Chardon, and L. Daudet, "Low frequency interpolation of room impulse responses using compressed sensing," *IEEE/ACM Transactions on Audio, Speech, and Language Processing*, vol. 22, no. 1, pp. 205–216, 2014.
- [14] D. L. Donoho, "Compressed sensing," *IEEE Transactions on Information Theory*, vol. 52, no. 4, pp. 1289–1306, 2006.
- [15] E. Candès, J. Romberg, and T. Tao, "Stable signal recovery from incomplete and inaccurate measurements," *Communications on Pure and Applied Mathematics*, vol. 59, no. 8, pp. 1207–1223, 2006.
- [16] F. Katzberg, R. Mazur, M. Maass, P. Koch, and A. Mertins, "Measurement of sound fields using moving microphones," *Proc. IEEE International Conference on Acoustics, Speech, and Signal Processing*, 2017, accepted.
- [17] T. I. Laakso, V. Välimäki, M. Karjalainen, and U. Laine, "Splitting the unit delay – tools for fractional delay filter design," *IEEE Signal Processing Magazine*, vol. 13, no. 1, pp. 30–60, 1996.
- [18] J. Allen and D. Berkley, "Image method for efficiently simulating small-room acoustics," *Journal of the Acoustical Society of America*, vol. 65, no. 4, pp. 943–950, 1979.
- [19] T. Knopp, S. Biederer, T. Sattel, J. Weizenecker, B. Gleich, J. Borgert, and T. M. Buzug, "Trajectory analysis for magnetic particle imaging," *Physics in Medicine and Biology*, vol. 54, no. 2, pp. 385–392, 2009.
- [20] A. P. Naylor and D. N. Gaubitch, "Subband inversion of multichannel acoustic systems," in *Speech Dereverberation*, pp. 189–217. London: Springer, 2010.
- [21] M. M. J. Yekta, "A frequency domain proof for the equivalence of the maximally flat FIR fractional delay filter and the lagrange interpolator," *Digital Signal Processing*, vol. 21, no. 1, pp. 13–19, 2011.